Available online at www.sciencedirect.com

ScienceDirect

International Journal of Solids and Structures 44 (2007) 2820–2836

INTERNATIONAL JOURNAL OF SOLIDS and STRUCTURES

www.elsevier.com/locate/ijsolstr

Multiple-zone sliding contact with friction on an anisotropic thermoelastic half-space

L.M. Brock [a], H.G. Georgiadis [b,*]

[a] *Department of Mechanical Engineering, University of Kentucky, Lexington, KY 40506, USA*
[b] *Mechanics Division, National Technical University of Athens, Zographou GR-15773, Greece*

Received 8 March 2006; received in revised form 8 July 2006
Available online 1 September 2006

Abstract

The paper studies a class of multiple-zone sliding contact problems. This class is general enough to include frictional and thermal effects, and anisotropic response of the indented material. In particular, a rigid die (indenter) slides with Coulomb friction and at constant speed over the surface of a deformable and conducting body in the form of a 2D half-space. The body is assumed to behave as a thermoelastic transversely isotropic material. Thermoelasticity of the Green–Lindsay type is assumed to govern. The solution method is based on integral transforms and singular integral equations. First, an exact transform solution for the auxiliary problem of multiple-zone (integer $n > 1$) surface tractions is obtained. Then, an asymptotic form for this auxiliary problem is extracted. This form can be inverted analytically, and the result applied to sliding contacts with multiple zones. For illustration, detailed calculations are provided for the case of two ($n = 2$) contact zones. The solution yields the contact zone width and location in terms of sliding speed, friction, die profile, and also the force exerted. Calculations for the hexagonal material zinc illustrate effects of speed, friction and line of action of the die force on relative contact zone size, location of maximal values for the temperature and the compressive stress, and the maximum temperature for a given maximum stress. Finally, from our general results, a single contact zone solution follows as a simple limit.

Keywords: Contact mechanics; Sliding contact problems; Thermal stresses; Anisotropic materials; Transverse isotropy; Integral transforms; Singular integral equations

1. Introduction

Models of sliding on planar surfaces of deformable bodies usually involve rigid dies (indenters) whose contours justify the assumption of single-zone contact (see e.g., Galin, 1961; Gladwell, 1980; Tabor, 1981). However, problems with *multiple* contact zones often arise in the mechanics of surfaces (see e.g., Ling, 1973; Hills and Nowell, 1994; Tichy and Meyer, 2000) and are worth studying. Standard multiple-zone contact analyses (see e.g., Kim and Kim, 2002) consider zones whose number, location and size are assumed, and whose trac-

* Corresponding author. Tel.: +30 210 7721365; fax: +30 210 7721302.
E-mail address: georgiad@central.ntua.gr (H.G. Georgiadis).

0020-7683/$ - see front matter
doi:10.1016/j.ijsolstr.2006.08.023

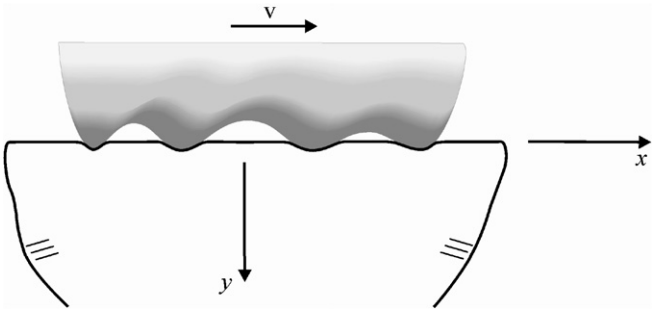

Fig. 1. Multiple-zone sliding contact.

tion distribution is specified to within an amplitude factor. The related sliding problem of two elastic surfaces, at least one of which has a low-amplitude wavy surface, often use periodic surface contours and contact zones of uniform width and either uniform traction distribution or uniformly distributed contact forces (Kuznetsov, 1985; Nosnovsky and Adams, 2000; Kim and Kim, 2002). Also, a 3D static analysis of normal contact by a rigid die without friction (Chekina and Keer, 1999) makes use of iterations to obtain the contact zone size in terms of the exerted load and die contour.

The present paper considers multiple-zone dynamic steady-state sliding with friction in plane-strain in which the number of zones ($n > 1$) can reasonably be assumed (see Fig. 1). The die profile (contour), friction and sliding speed, and specification of how die force is distributed determine zone size and location, and whether or not the zone number is less than that assumed. Contrary to the procedure of Chekina and Keer (1999), an analytical *non-iterative* solution scheme is followed here.

Our problem involves a rigid die that slides on a 2D half-space at constant speed below the speed of Rayleigh waves (sub-critical speed). The half-space responds as a linear, homogeneous, thermoelastic transversely isotropic solid. In order to reduce the problem to a set of integral equations, an exact integral-transform solution for an auxiliary problem is first developed. This problem involves *only* tractions specified on $n > 1$ translating surface zones. Robust asymptotic forms are extracted that allow transform inversions to be done analytically. It turns out that thermal relaxation effects are negligible and classical Fourier heat conduction governs. Then, the inversions are applied to the original sliding contact problem, whose number of contact zones is assumed to be $n > 1$. An exact general solution is obtained, and detailed calculations are presented for illustration for the case $n = 2$ and the hexagonal material zinc at room temperature. The results show effects of sliding speed, friction and die force system on contact zone size and thermal response.

2. Basic equations in plane-strain

In terms of Cartesian coordinates (x, y, z), consider a linear, homogeneous thermoelastic half-space $y > 0$ (see Fig. 1). The half-space is transversely isotropic, with its surface and surface normal defining, respectively, the plane and axis of material symmetry. The half-space is at rest and at uniform (absolute) temperature T_0 when a surface disturbance generates a state of plane-strain in (x, y). The theory of generalized thermoelasticity of Green and Lindsay (1972) is adopted here. According to this theory, the field equations in the absence of body forces and heat sources are written as (see also Dhaliwal and Sherief, 1980; Sharma and Sharma, 2002)

$$\partial_x \sigma_{xx} + \partial_y \sigma_{xy} = \rho \ddot{u}_x, \quad \partial_x \sigma_{xy} + \partial_y \sigma_{yy} = \rho \ddot{u}_y \tag{1a, b}$$

$$K_x \partial_x^2 \theta + K_y \partial_y^2 \theta - \rho c_v D_0(\dot{\theta}) - T_0 D_1(\beta_x \dot{u}_x + \beta_y \dot{u}_y) = 0 \tag{1c}$$

whereas the constitutive equations are given by

$$\begin{bmatrix} \sigma_{xx} \\ \sigma_{yy} \\ \sigma_{zz} \end{bmatrix} = \begin{bmatrix} c_{11} & c_{12} & c_{13} \\ c_{12} & c_{22} & c_{12} \\ c_{13} & c_{12} & c_{11} \end{bmatrix} \begin{bmatrix} \partial_x u_x - \alpha_x D_1(\theta) \\ \partial_y u_y - \alpha_y D_1(\theta) \\ -\alpha_x D_1(\theta) \end{bmatrix}, \quad \sigma_{xy} = c_{44}(\partial_x u_y + \partial_y u_x) \tag{2a, b}$$

In the above equations, (∂_x, ∂_y) denote (x,y)-differentiation, a superposed dot denotes time differentiation, (u_x, u_y) are the displacements, θ is the temperature change, $(\sigma_{xx}, \sigma_{xy}, \sigma_{yy}, \sigma_{zz})$ are components of the stress tensor, ρ is the mass density, $(c_{11}, c_{12}, c_{13}, c_{22}, c_{44})$ are the elastic constants, c_v is the specific heat at constant volume, (α_x, α_y) are coefficients of thermal expansion, (K_x, K_y) are coefficients of thermal conductivity, and

$$D_0(f) = f + \tau_0 \dot{f}, \quad D_1(f) = f + \tau_1 \dot{f} \tag{3a, b}$$

$$\beta_x = \alpha_x(c_{11} + c_{13}) + \alpha_y c_{12}, \quad \beta_y = 2\alpha_x c_{12} + \alpha_y c_{22} \tag{4a, b}$$

where (τ_0, τ_1) are thermal relaxation times, and $D_0(\,)$ and $D_1(\,)$ are corresponding thermal relaxation operators. Due to thermodynamic restrictions, the material constants should obey the following constraints (Chadwick, 1960; Green and Lindsay, 1972; Payton, 1983)

$$c_{11} \geqslant |c_{13}|, \quad (c_{11} + c_{13})c_{22} > 2c_{12}^2, \quad c_{44} > 0, \quad \rho > 0 \tag{5a}$$

$$(\alpha_x, \alpha_y) > 0, \quad (K_x, K_y) > 0, \quad c_v > 0, \quad \tau_0 \geqslant \tau_1 \geqslant 0 \tag{5b}$$

Finally, it is noted that the plane-strain equations of a simpler version of generalized thermoelasticity by Lord and Shulman (1967) – a theory involving one relaxation time – result as a special case of the above equations by having the operator $D_1(\,)$ in (1c) being replaced by $D_0(\,)$ and the term $D_1(\theta)$ in (2a) being replaced simply by θ.

3. Basic integral-transform analysis

In this section, we will obtain a transform solution to a problem that is *auxiliary* to the original contact problem. Such a strategy was followed before by the present authors in dealing with problems involving a single contact zone (Brock and Georgiadis, 2000, 2001). The present auxiliary problem involves plane-strain surface disturbances caused by normal and shear tractions applied to multiple ($n > 1$) zones of fixed width that translate in the positive x-direction at constant sub-critical speed V. It is also assumed that the tractions do not vary with time, and therefore, after a certain time, a dynamic steady-state will be reached. If a moving Cartesian coordinate system is considered that is translated with the same velocity, it then follows from the *steady-state* assumption and the well-known Galilean transformation that $\dot{f} = -V\partial_x f$, where f is any field quantity, and (u_x, u_y, θ) depend only on (x,y) (see e.g., Brock and Georgiadis, 1997). Boundary conditions along the surface $(y = 0)$ are written as

$$(\sigma_{xy}, \sigma_{yy}) = 0 \ \ (x \notin Z_i), \quad (\sigma_{xy}, \sigma_{yy}) = (\sigma_S^i, \sigma_N^i) \ \ (x \in Z_i), \quad \partial_y \theta = 0 \tag{6a, b, c}$$

where $i = (1, 2, \ldots, n)$, $\sigma_N^i(x)$ and $\sigma_S^i(x)$ are normal and shear tractions, and Z_i are the translating zones of fixed width L_i. With respect to direction of motion, Z_1 is the trailing zone and Z_n is the leading one. The condition in (6c) reflects the assumption that surface convection is negligible. Finally, the pertinent finiteness conditions at remote regions require that (u_x, u_y, θ) be bounded at $\sqrt{x^2 + y^2} \to \infty$.

We now introduce several quantities that serve the purpose of convenient normalizations. These are a pseudo-rotational wave speed (as is well-known, in anisotropic materials there are no waves of pure rotation and dilatation – see e.g., Payton, 1983) v_r, the average expansion coefficient α and three thermoelastic characteristic lengths (h, h_0, h_1)

$$v_r = \sqrt{\frac{c_{44}}{\rho}}, \quad \alpha = \frac{1}{2}(\alpha_x + \alpha_y), \quad h = \frac{K_x + K_y}{2\rho c_v v_r}, \quad h_0 = v_r \tau_0, \quad h_1 = v_r \tau_1 \tag{7}$$

The following dimensionless parameters serve also the same purpose:

$$(C_x, C_y) = 2\frac{(K_x, K_y)}{K_x + K_y}, \quad c = \frac{V}{V_r}, \quad \varepsilon = \frac{T_0}{c_v}(\alpha v_r)^2 \tag{8a}$$

$$a = \frac{c_{22}}{c_{44}}, \quad b = \frac{c_{11}}{c_{44}}, \quad m = 1 + \frac{c_{12}}{c_{44}}, \quad m_3 = 1 + \frac{c_{13}}{c_{44}}, \quad \gamma = 1 + ab - m^2 \tag{8b}$$

$$\alpha\Gamma_x = (b + m_3 - 1)\alpha_x + (m - 1)\alpha_y, \quad \alpha\Gamma_y = 2(m - 1)\alpha_x + a\alpha_y \tag{8c}$$

We should notice at this point that, for most engineering materials, quantities defined above have the following orders of magnitude (Chadwick, 1960; Achenbach, 1973; Sharma and Sharma, 2002):

$$h = \mathrm{O}(10^{-9}\ \mathrm{m}), \quad \varepsilon = \mathrm{O}(10^{-2}), \quad v_r = \mathrm{O}(10^{3}\ \mathrm{m/s}), \quad (\tau_0, \tau_1) = \mathrm{O}(10^{-13}\ \mathrm{s}) \tag{9}$$

from which it follows that $h > h_0 > h_1$.

The steady-state boundary value problem will be attacked by the two-sided Laplace transform (see e.g., van der Pol and Bremmer, 1950; Bracewell, 1965) over the x-variable in order to suppress dependence of the field equations and the boundary conditions upon this variable. The direct and inverse operations are defined as

$$\hat{f}(p,y) = \int_{-\infty}^{\infty} f(x,y)\mathrm{e}^{-px}\,\mathrm{d}x, \quad f(x,y) = \frac{1}{2\pi\mathrm{i}}\int_{Br} \hat{f}(p,y)\mathrm{e}^{px}\,\mathrm{d}p \tag{10a, b}$$

where the variable p is in general complex and Br denotes the Bromwich path of inversion in the p-plane (i.e., a line parallel to the imaginary axis *within* the strip of analyticity of $\hat{f}(p,y)$). Application of the direct transform to (6) and the steady-state forms of (1)–(4) gives, after some rather involved algebra, the following results written in compact form:

$$p\hat{u}_x = \alpha d_0' \sum_{k=1}^{3} (\Gamma_x B^2 + K_y q_k^2) Q_k \exp(-pq_k y) \tag{11a}$$

$$p\hat{u}_y = -\alpha d_1' \sum_{k=1}^{3} (K_x + \Gamma_y q_k^2) q_k Q_k \exp(-pq_k y) \tag{11b}$$

$$\hat{\theta} = a \sum_{k=1}^{3} (q_k^4 + C q_k^2 + A^2 B^2) Q_k \exp(-pq_k y) \tag{11c}$$

where $y > 0$ (which is the case of interest) and the coefficients Q_k are given by

$$Q_k = \frac{a}{\alpha Q}(q_i - q_j)\left[\frac{\hat{\sigma}_{\mathrm{S}}}{c_{44}} H(q_i, q_j) + \frac{\hat{\sigma}_{\mathrm{N}}}{c_{44}} q_i q_j (q_i + q_j) G(q_i, q_j)\right] \tag{12a}$$

with

$$Q = -\sum_{k=1}^{3} (M_y q_k^2 + N_x B^2) q_i q_j (q_i^2 - q_j^2) G(q_i, q_j) \tag{12b}$$

$$(\hat{\sigma}_{\mathrm{N}}, \hat{\sigma}_{\mathrm{S}}) = \sum_{i=1}^{n} \int_{Z_i} (\sigma_{\mathrm{N}}^i, \sigma_{\mathrm{S}}^i)\mathrm{e}^{-p\omega}\,\mathrm{d}x\omega. \tag{12c}$$

In (12a) and (12b), (i,j,k) cycle through $(1,2,3)$, but with $i \neq j \neq k$. For example, the indices may have the values $(i = 1, j = 2, k = 3)$. Also, in (12c), the integration is taken over each interval Z_i. In (12a) and (12b), the dimensionless functions

$$G(\xi,\eta) = M_x(\xi^2 + \eta^2 + C) + N_y(\xi^2\eta^2 - A^2B^2) \tag{13a}$$

$$H(\xi,\eta) = -N_x B^2(\xi^2 + \eta^2 + \xi\eta)(\xi^2 + \eta^2 + C) + A^2B^2(M_y\xi\eta - N_x B^2) + \xi^2\eta^2[N_x B^2 - M_y(\xi^2 + \eta^2 + \xi\eta)] \tag{13b}$$

are symmetric in (ξ,η), and dimensionless terms are given as

$$M_r = k_r + \Gamma_r B^2, \quad N_r = k_r + \Gamma_r \quad \text{with } r = (x,y) \tag{14a}$$

$$k_x = (b - c^2)\Gamma_y - m\Gamma_x, \quad k_y = a\Gamma_x - m\Gamma_y \tag{14b}$$

As indicated in (11a) and (11b), dimensionless thermal relaxation factors

$$d_0' = 1 - ch_0 p, \quad d_1' = 1 - ch_1 p \tag{15}$$

also arise, where in the limit cases considered by Lord and Shulman (1967) and Sharma and Sharma (2002) it is set, respectively, $d_1' = 1$ and $d_0' = 1$. Finally, q_k^2 are dimensionless cubic roots of the equation

$$q^6 + \left(\alpha_2 + \frac{\beta_2}{hp}\right)q^4 + \left(\alpha_1 + \frac{\beta_1}{hp}\right)q^2 + \left(\alpha_0 + \frac{\beta_0}{hp}\right)B^2 = 0 \tag{16}$$

where the coefficients in (16) are given by

$$\alpha_0 = k_c A^2 - k_h A_h^2 c^2, \quad \beta_0 = k_\varepsilon A_\varepsilon c \tag{17a}$$

$$\alpha_1 = A^2 B^2 + k_c C - k_h C_h c^2, \quad \beta_1 = k_\varepsilon C_\varepsilon c \tag{17b}$$

$$\alpha_2 = C + k_c - k_h c^2, \quad \beta_2 = k_\varepsilon c \tag{17c}$$

The above terms and those in (11)–(14) exhibit the following parameters:

$$k_c = \frac{C_x}{C_y}, \quad k_\varepsilon = \frac{a_\varepsilon}{aC_y}, \quad k_h = \frac{h_0}{h}\frac{a_h}{aC_y} \tag{18a}$$

$$C = \Delta + A^2 + B^2, \quad \sqrt{a}A = \sqrt{b - c^2}, \quad a\Delta = (a-1)(b-1) - m^2, \quad B = \sqrt{1 - c^2} \tag{18b}$$

$$C_\varepsilon = \Delta_\varepsilon + A_\varepsilon^2 + B^2, \quad \sqrt{a_\varepsilon}A_\varepsilon = \sqrt{b_\varepsilon - c^2}, \quad a_\varepsilon\Delta_\varepsilon = (a_\varepsilon - 1)(b_\varepsilon - 1) - m_\varepsilon^2 \tag{18c}$$

$$C_h = \Delta_h + A_h^2 + B^2, \quad \sqrt{a_h}A_h = \sqrt{b_h - c^2}, \quad a_h\Delta_h = (a_h - 1)(b_h - 1) - m_h^2 \tag{18d}$$

In (18), the following dimensionless constants are defined:

$$a_\varepsilon = a + \varepsilon_x, \quad b_\varepsilon = b + \varepsilon_y, \quad m_\varepsilon = m + \sqrt{\varepsilon_x \varepsilon_y}, \quad \gamma_\varepsilon = 1 + a_\varepsilon b_\varepsilon - m_\varepsilon^2 \tag{19a}$$

$$a_h = a + \frac{h'}{h_0}\varepsilon_x, \quad b_h = b + \frac{h'}{h_0}\varepsilon_y, \quad m_h = 1 + \frac{h'}{h_0}\sqrt{\varepsilon_x \varepsilon_y}, \quad \gamma_h = 1 + a_h b_h - m_h^2 \tag{19b}$$

$$\varepsilon_r = \varepsilon \Gamma_r^2 \quad \text{with } r = (x, y) \tag{19c}$$

The $(\varepsilon_x, \varepsilon_y)$ are dimensionless thermoelastic coupling constants for transverse isotropy, and in the limit cases considered by Lord and Shulman (1967) and Sharma and Sharma (2002) it is set $h' = h_0$ and $h' = h_1$, respectively. The terms in (14a) and (14b) are invariant under transformations $(a, b, m) \to (a_\varepsilon, b_\varepsilon, m_\varepsilon) \to (a_h, b_h, m_h)$. It is also noted that $(\Delta, \Delta_\varepsilon, \Delta_h) = 0$ in the isotropic limit. Finally, standard results for a cubic equation (see e.g., Abramowitz and Stegun, 1972) can be used to write formal expressions for (q_1^2, q_2^2, q_3^2) in terms of (17).

4. Asymptotic results for the auxiliary problem

In view of the complicated form of the transformed solution (11) given before, it seems that numerical inversion is the only possibility. Notice that numerical inversion of Laplace transforms is a procedure with a lot of difficulty. However, past experience with analogous forms in thermoelastic problems (Brock and Georgiadis, 1997, 1999, 2000; Brock, 2003, 2004) shows that an asymptotic *analytical* approach can still be possible. This approach follows from the Tauberian theorems on Laplace transforms (van der Pol and Bremmer, 1950; Berg, 1967) and is based on the observation that, in view of (10), a transform approximation valid for $|hp| \ll 1$ will give an inversion valid for $|x/h| \gg 1$. The first relation in (9) implies that such an inversion is robust indeed. For example, any case where $|x/h| > 1000$ will lead to a reasonable approximation, so we consider here the interval $\mathrm{O}(10^{-6}\,\mathrm{m}) < |x| < \infty$ to be the range of validity. Therefore, transform-related expressions presented above are expanded for small $|hp|$ and only the lowest-order terms are kept. Thus

$$(q_1, q_2, q_3) = \left(A', B', \frac{1}{\sqrt{h_\varepsilon p}}\right)\frac{\sqrt{-p}}{\sqrt{p}} \tag{20}$$

where $\sqrt{-p}$ and $\sqrt{p}$ can be viewed as, respectively, the functions $\sqrt{\tau - p}$ and $\sqrt{\tau + p}$ with τ a real number such that $\tau \to +0$ (the latter forms facilitate the introduction of the pertinent branch cuts in complex p-plane). Length h_ε and dimensionless parameters (A', B') are given by (18c) and

$$h_\varepsilon = \frac{h}{k_\varepsilon c}, \quad A' = \Omega + \omega, \quad B' = \Omega - \omega \tag{21a}$$

$$2\Omega = \sqrt{\Delta_\varepsilon + (A_\varepsilon + B)^2}, \quad 2\omega = \sqrt{\Delta_\varepsilon + (A_\varepsilon - B)^2}, \quad A'B' = A_\varepsilon B \tag{21b}$$

It is worthwhile noticing at this point that the absence of thermal characteristic lengths (h_0, h_1) in the above equations clearly shows that thermal relaxation is negligible for this asymptotic expansion, i.e., only classical Fourier heat flow (Boley and Weiner, 1985) governs the thermal field. Then (11a) gives, for example,

$$p\hat{u}_x = \frac{\exp(-A'y\sqrt{-p}\sqrt{p})}{(B'-A')R}\left(N_A\frac{\hat{\sigma}_N}{c_{44}} - BU_B\frac{\sqrt{-p}}{\sqrt{p}}\frac{\hat{\sigma}_S}{c_{44}}\right) + \frac{\exp(-B'y\sqrt{-p}\sqrt{p})}{(B'-A')R}\left(N_B\frac{\hat{\sigma}_N}{c_{44}} - BU_A\frac{\sqrt{-p}}{\sqrt{p}}\frac{\hat{\sigma}_S}{c_{44}}\right) \tag{22}$$

where dimensionless parameters that appear are given by

$$(N_A, N_B) = a_\varepsilon A_\varepsilon(A', B') + (m_\varepsilon - 1)(B', A') \tag{23a}$$

$$(U_A, U_B) = m_\varepsilon(m_\varepsilon - 1) - a_\varepsilon^2 A_\varepsilon^2 + a_\varepsilon(A'^2, B'^2) \tag{23b}$$

$$R = -a_\varepsilon c^2 A_\varepsilon + [a_\varepsilon^2 A_\varepsilon^2 - (m_\varepsilon - 1)^2]B \tag{23c}$$

Quantity R above is a *Rayleigh-type* form (i.e., a form corresponding to the existence of a certain type of *generalized* Rayleigh waves – specifically, transversely isotropic thermoelastic surface waves). Finally, the dimensionless quantity D is defined

$$D = \Gamma_x\Gamma_y B^2 - k_x k_y \equiv c^{-2}(N_x N_y B^2 - M_x M_y) \tag{24}$$

where, like the quantities $(\Delta, \Delta_\varepsilon, \Delta_h)$, D vanishes in the isotropic limit.

Now, material characterization for the present case of *thermal* transverse isotropy may follow in an analogous manner of the isothermal transverse isotropy (Payton, 1983). In our case, we have

$$\begin{aligned}
&\text{Category 1}: \quad 2\sqrt{a_\varepsilon b_\varepsilon} \leqslant \gamma_\varepsilon \leqslant 1 + a_\varepsilon b_\varepsilon, \quad 1 < b_\varepsilon < a_\varepsilon\\
&\qquad\qquad\quad a_\varepsilon + b_\varepsilon \leqslant \gamma_\varepsilon \leqslant 1 + a_\varepsilon b_\varepsilon, \quad 1 < a_\varepsilon < b_\varepsilon\\
&\qquad\qquad\quad 2a_\varepsilon \leqslant \gamma_\varepsilon \leqslant 1 + a_\varepsilon^2, \quad 1 < b_\varepsilon = a_\varepsilon\\
&\text{Category 2}: \quad 1 + b_\varepsilon < \gamma_\varepsilon < a_\varepsilon + b_\varepsilon, \quad \gamma_\varepsilon^2 - 4a_\varepsilon b_\varepsilon < 0\\
&\text{Category 3}: \quad \gamma_\varepsilon < 1 + b_\varepsilon, \gamma_\varepsilon^2 - 4a_\varepsilon b_\varepsilon < 0.
\end{aligned}$$

Further, an inspection shows that for speeds in the range $0 < v < c_0 v_r$, Ω in a material belonging to Category 3 remains positive real on the Re(c)-axis, but (A', B') are now complex conjugates

$$\mathrm{Im}(c) = 0\pm, \quad 0 < |c| < c_0: \quad A' = \Omega \mp \mathrm{i}\bar{\omega}, \quad B' = \Omega \pm \mathrm{i}\bar{\omega}, \qquad \bar{\omega} = \sqrt{-\Delta_\varepsilon - (A_\varepsilon - B)^2} \tag{25}$$

Notice that the dimensionless speed

$$c_0 = \sqrt{1 - \left(\frac{a_\varepsilon\sqrt{-\Delta_\varepsilon} - m_\varepsilon}{a_\varepsilon - 1}\right)^2} < 1 \tag{26}$$

vanishes in the isotropic limit. In addition, in this limit $(A', B') \to (A_\varepsilon, B)$.

Study of (23c) also shows that

$$R(0) > 0, \quad R(\pm 1) < 0, \quad R(\pm c_R) = 0 \ \ (0 < c_R < 1). \tag{27}$$

Thus $c_R v_r$ is the Rayleigh speed in the material symmetry plane. To avoid singular behavior in (22), the value $c = c_R$ is excluded from the range of the subsonic speeds of the surface disturbance. In view of this, inversions of (22) and $(p\hat{u}_y, \hat{\theta})$ were derived and the results are assembled in Appendix A (analogous results were derived in the work by Brock, 2004). These results for the auxiliary problem will be applied next to the sliding contact problem.

5. Application to sliding contact: solution candidate

Consider the $n > 1$ moving surface zones to be imposed by translation of a rigid die with speed V. Condition (6) for $y = 0$ is now replaced by the following mixed condition:

$$(\sigma_{xy},\sigma_{yy})=0\ \ (x\notin Z_i),\quad \sigma_{xy}=\mu_i\sigma_{yy},\quad \partial_x u_y=\frac{\mathrm{d}V_i}{\mathrm{d}x}\ \ (x\in Z_i),\quad \partial_y\theta=0 \tag{28}$$

In each contact zone Z_i, μ_i is the friction coefficient and $V_i(x)$ is the imposed normal displacement (indenter profile). The indenter profile is smooth enough to ensure that the functions $(V_i, \mathrm{d}V_i/\mathrm{d}x, \mathrm{d}^2V_i/\mathrm{d}x^2)$ are all bounded and continuous in Z_i. Comparison of (6) and (28) shows, in view of (A.1b) and (A.3b) (see Appendix A) and the following representation of the Dirac delta distribution (see e.g., van der Pol and Bremmer, 1950; Bracewell, 1965)

$$\lim_{\eta\to+0}\delta(\xi)=\frac{1}{\pi}\frac{\eta}{\xi^2+\eta^2} \tag{29}$$

that the previous moving traction-zone results provide a solution candidate for sliding contact if

$$\sigma_{\mathrm{S}}^i=\mu_i\sigma_i(x),\quad \sigma_{\mathrm{N}}^i=\sigma_i(x)\qquad (x\in Z_i) \tag{30a}$$

$$\frac{\mu_i M_+}{R}\frac{\sigma_i}{c_{44}}+\frac{2a_e A_e\Omega}{\pi R}\sum_{k=1}^{n}\int_{Z_k}\frac{\sigma_k}{c_{44}}\frac{\mathrm{d}t}{t-x}=\frac{\mathrm{d}V_i}{\mathrm{d}x}\quad (x\in Z_i) \tag{30b}$$

In particular, integration for the term $k=i$ is taken in the Cauchy principal value sense. The set (30b) of singular integral equations (see e.g., Carrier et al., 1966; Erdogan, 1976) can, after the work of Brock and Georgiadis (2000) and Brock (2003), be solved to yield for $x\in Z_i$

$$\frac{\sigma_i}{c_{44}}=R\left[\frac{\mathrm{d}V_i}{\mathrm{d}x}\frac{\cos\pi\upsilon_i}{S_i}+\Pi_k^n\left|\frac{x-L_k^+}{x-L_k^-}\right|^{\upsilon_k}\frac{\sin\pi\upsilon_i}{\pi}\sum_{k=1}^{n}\frac{1}{S_k}\int_{Z_k}\Pi_j^n\left|\frac{t-L_j^-}{t-L_j^+}\right|^{\upsilon_j}\frac{\mathrm{d}V_k}{\mathrm{d}t}\frac{\mathrm{d}t}{t-x}\right] \tag{31}$$

Principal value integration is again necessary for the term $k=i$, Π_k^n implies the product of factors indexed by k over range $k=1,2,\ldots n$, and

$$S_i=\sqrt{(\mu_i M_+)^2+(2a_e A_e\Omega)^2},\quad \upsilon_i=-\frac{1}{2}+\frac{1}{\pi}\tan^{-1}\frac{\mu_i M_+}{2a_e A_e\Omega}\quad\left(-\frac{1}{2}<\upsilon_i<0\right) \tag{32}$$

The υ_i are eigenvalues of the integral equation set, and $x=L_i^{\pm}$ locate, respectively, the leading and trailing edges of contact zone Z_i. They are not given from the problem statement, although subject to non-overlap constraints

$$L_i^+-L_i^-=L_i>0\quad (i=1,2,\ldots n),\qquad L_{i+1}^->L_i^+\quad (i=1,2,\ldots n-1) \tag{33}$$

In order to be the contact problem solution, candidate set (31) must satisfy certain additional conditions, and these should allow determination of $(L_i^{\pm},L_i)$. More specifically, these conditions stem from the *Signorini* inequalities for contact problems and the constraint of negative rate of frictional work.

First, as the work of Georgiadis and Barber (1993) generally showed, the smoothness requirements for $V_i(x)$ should preclude singular behavior at the contact zone edges (in fact, contact stresses should tend to zero continuously when a zone edge is approached). This constraint of smooth contact stresses, in the case of smooth $V_i(x)$, guarantees that there will be *no* interpenetration between indenter and half-space material outside the contact zones (first Signorini condition). Vanishing of the contact stress, in turn, implies the following conditions at $x=L_i^+$ for the set (31) (see e.g., Erdogan, 1976)

$$\sum_{k=1}^{n}\frac{1}{S_k}\int_{Z_k}\Pi_j^n\left|\frac{t-L_j^-}{t-L_j^+}\right|^{\upsilon_j}\frac{\mathrm{d}V_k}{\mathrm{d}t}\frac{\mathrm{d}t}{L_i^+-t}=0\quad (i=1,2\ldots n) \tag{34}$$

Then, considering equilibrium, i.e., specifying the resultant force system exerted by the die on the half-space, and $n-2$ requirements related to how the resultant force is distributed, gives the following n conditions:

$$\sum_i^n \int_{Z_i} \sigma_i \,\mathrm{d}t + F = 0, \quad \sum_i^n \int_{Z_i} t\sigma_i \,\mathrm{d}t + M_0 = 0 \tag{35a}$$

$$\int_{Z_k} \sigma_k \,\mathrm{d}t + F_k = 0 \quad (k = 2, 3 \ldots n-1), \quad \sum_k^n F_k = F \tag{35b}$$

Here F is the total compressive force (per unit length in the z-direction), M_0 is the clockwise moment (per unit length in the z-direction) about $(x = 0, y = 0)$, and F_k is the portion of F assumed to be borne by zone Z_k. Substitution of (31) into (35a) and use of contour integration and Cauchy's theorem produces the following more explicit forms:

$$c_{44}R \sum_{i=1}^n \frac{1}{S_i} \int_{Z_i} \Pi_k^n \left| \frac{t - L_k^-}{t - L_k^+} \right|^{\upsilon_k} \frac{\mathrm{d}V_i}{\mathrm{d}t} \mathrm{d}t + F = 0 \tag{36a}$$

$$c_{44}R \sum_{i=1}^n \frac{1}{S_i} \int_{Z_i} \Pi_k^n \left| \frac{t - L_k^-}{t - L_k^+} \right|^{\upsilon_k} \frac{\mathrm{d}V_i}{\mathrm{d}t} t \,\mathrm{d}t = M_0 + F \sum_{i=1}^n \upsilon_i L_i \tag{36b}$$

Now, if it is also assumed that the width of any contact zone is *much* smaller than the separation between any two adjacent zones, introducing the integration variable

$$t = \widetilde{L}_i + \frac{1}{2} L_i u, \quad \widetilde{L}_i = \frac{1}{2}(L_i^+ + L_i^-) \tag{37}$$

in (31), (34), (35b) and (36) and recognizing that

$$L_i \ll L_{k+1}^- - L_k^+ \quad (i, k = 1, 2 \ldots n) \tag{38}$$

gives the robust *approximations*

$$\sum_i^n \frac{1}{2S_i} \int_{-1}^1 \left(\frac{u+1}{1-u} \right)^{\upsilon_i} \frac{\mathrm{d}V_i}{\mathrm{d}x} (\widetilde{L}_i + \frac{1}{2}u) \frac{\mathrm{d}u}{1-u} \approx 0 \quad (i = 1, 2 \ldots n) \tag{39a}$$

$$c_{44}R \sum_i^n \frac{L_i}{2S_i} \int_{-1}^1 \left(\frac{u+1}{1-u} \right)^{\upsilon_i} \frac{\mathrm{d}V_i}{\mathrm{d}x} \left(\widetilde{L}_i + \frac{1}{2} L_i u \right) \mathrm{d}u + F \approx 0 \tag{39b}$$

$$c_{44}R \sum_i^n \frac{L_i}{2S_i} \int_{-1}^1 \left(\frac{u+1}{1-u} \right)^{\upsilon_i} \left(\widetilde{L}_i + \frac{1}{2} L_i u \right) \frac{\mathrm{d}V_i}{\mathrm{d}x} \left(\widetilde{L}_i + \frac{1}{2} L_i u \right) \mathrm{d}u \approx M_0 + F \sum_i^n \upsilon_i L_i \tag{39c}$$

$$c_{44} \frac{RL_k}{2S_k} \int_{-1}^1 \left(\frac{u+1}{1-u} \right)^{\upsilon_k} \frac{\mathrm{d}V_k}{\mathrm{d}x} \left(\widetilde{L}_k + \frac{1}{2} L_k u \right) \mathrm{d}u + F_k \approx 0 \quad (k = 2, 3 \ldots n-1) \tag{39d}$$

It is noted that integration is now with respect to a dimensionless variable, that the contact zone width/location parameters appear explicitly only in the argument of specified functions, and that $x = \widetilde{L}_i$ is the center of each contact zone. More importantly, the parameter sets $(L_i, \widetilde{L}_i)$ for the contact zones Z_i are *uncoupled* in (39).

Finally, the second Signorini condition states that the contact zones cannot sustain tension (see e.g., Georgiadis and Barber, 1993), whereas the last inequality pertains to the physical requirement that frictional work rate cannot be positive

$$\sigma_i \leqslant 0, \quad \mu_i \sigma_i (V - \dot{u}_x) \leqslant 0 \quad (x \in Z_i) \tag{40}$$

In view of the first requirement in (37) the second is reduced in a steady-state situation to

$$1 + \partial_x u_x \geqslant 0 \quad (x \in Z_i) \tag{41}$$

Construction of a complete solution is now illustrated for a problem of two-zone contact.

6. An example: two-zone contact

Consider a 'rounded W' rigid indenter (die) depicted in Fig. 2 and defined in the moving coordinates by the fourth-order polynomial

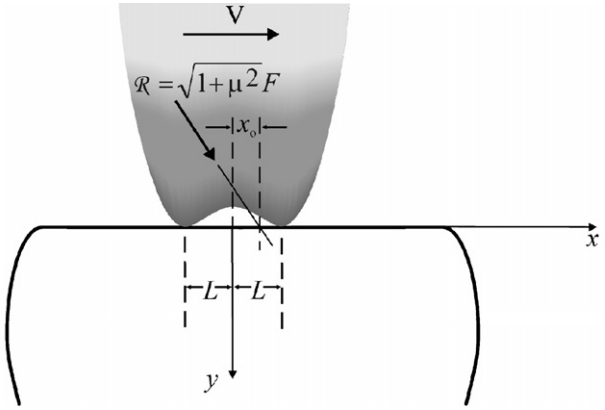

Fig. 2. A 'rounded W' rigid die sliding with speed V and its resultant force $\Re$ on half-space.

$$y = \frac{x^2}{2L^2}\left(1 - \frac{x^2}{2L^2}\right) - \frac{L}{4} \tag{42}$$

where, in accord with the asymptotic Laplace-transform inversion in Section 4, it is assumed that $L \gg h$. Contact is assumed to occur about the die bases ($x = \pm L$, $y = 0$), and frictional properties in the zones are taken identical. Thus,

$$\mu_i = \mu, \quad \frac{\mathrm{d}V_i}{\mathrm{d}x} = \frac{x}{L}\left(1 - \frac{x^2}{L^2}\right) \qquad (i = 1, 2) \tag{43a}$$

$$S_i = S = \sqrt{(\mu M_+)^2 + (2a_\varepsilon A_\varepsilon \Omega)^2}, \quad \upsilon_i = \upsilon = -\frac{1}{2} + \frac{1}{\pi}\tan^{-1}\frac{\mu M_+}{2a_\varepsilon A_\varepsilon \Omega} \qquad (i = 1, 2) \tag{43b}$$

To illustrate their advantages, we for the moment neglect approximation (39). Thus, combining (31), (34) and (43) and using contour integration and Cauchy's theorem gives

$$\frac{\sigma_i}{c_{44}} = \frac{-R}{L^3 S}\left(\frac{L_2^+ - x}{x - L_1^-}\right)^{\upsilon}\left|\frac{L_1^+ - x}{L_2^- - x}\right|^{\upsilon}(x - L_1^+)(x - L_2^+)(x + L_1^+ + L_2^+ + \upsilon L_Z) \quad (x \in Z_i) \tag{44a}$$

$$(L_i^+ + \upsilon L_Z)[L^2 - L_i^{+2} + \upsilon(L_1 L_2^+ + L_2 L_1^+)] + \frac{\upsilon}{2}L_i^+(L_1^2 + L_2^2 - \upsilon L_Z^2) - \frac{\upsilon}{3}(1 - \upsilon)(L_1^3 + L_2^3 - \upsilon L_Z^3) - \upsilon(L_1 L_1^+ L_1^- + L_2 L_2^+ L_2^-) = 0 \quad (i = 1, 2) \tag{44b}$$

$$L_Z = L_1 + L_2, \quad L_i^- = L_i^+ - L_i \quad (i = 1, 2) \tag{44c}$$

If (38) is now imposed then (44b) gives the two valid approximations

$$L + L_i^+ + \upsilon L_i \approx 0 \quad (i = 1, 2) \tag{45}$$

Use of (39a) gives, of course, the same results directly. Result (44a) satisfies the first constraint in (40) when

$$0 < c < c_{\mathrm{R}} \tag{46}$$

In complete accord with the analyses by Georgiadis and Barber (1993) and Brock and Georgiadis (2000), this range defines, therefore, *sub-critical* sliding speed. In other words, we restrict the indenter velocity to be in this range in order to avoid non-uniqueness and instability of solution candidates.

Because $n = 2$, auxiliary condition (35b) and its robust approximation (39d) need not be considered. In view of (45), we use approximation (39b) and (39c): substitution of (42) and use of contour integration and Cauchy's theorem gives

$$\frac{\pi\upsilon R}{2a_\varepsilon A_\varepsilon \Omega}\left[(1+\upsilon)(L_1^2+L_2^2)+\upsilon L_1 L_2\right]+\frac{FL}{c_{44}}\approx 0 \tag{47a}$$

$$\frac{\pi\upsilon R}{2a_\varepsilon A_\varepsilon \Omega}(1+\upsilon)(L_1^2-L_2^2)+\frac{M_0}{c_{44}}\approx 0 \tag{47b}$$

As depicted in Fig. 2, the line of action of resultant force $\Re=\sqrt{1+\mu^2}F$ and its point of intersection with the half-space surface, respectively, are

$$x-\mu y=\frac{M_0}{F},\quad x_0=\frac{M_0}{F} \tag{48}$$

Solutions to coupled equations (47) can be written in terms of (F,x_0) as

$$(L_2^2,L_1^2)\approx\frac{-a_\varepsilon A_\varepsilon\Omega}{2\pi\upsilon(1+\upsilon)R}\frac{FL}{c_{44}}\left[(\sqrt{s_\upsilon^2-s^2}-\sqrt{s_\upsilon^2-1})^2+(s\pm 1)^2\right] \tag{49a}$$

$$s=\frac{x_0}{L}(|s|<1),\quad s_\upsilon=\frac{2(1+\upsilon)}{\sqrt{4(1+\upsilon)^2-\upsilon^2}}>1 \tag{49b}$$

The restriction on s guarantees both non-negative (49a), and in view of Fig. 2, (38) and (48), that the line of action must pass between the die bases. Limit cases $s=\pm 1$ correspond to $(L_1\approx 0, L_2\approx L^*)$ and $(L_2\approx 0, L_1\approx L^*)$, respectively, i.e., when single-zone contact occurs. Here, L^* is the maximum width in this limit, and is given by

$$L^{*2}\approx-\frac{2a_\varepsilon A_\varepsilon\Omega}{\pi\upsilon(1+\upsilon)R}\frac{FL}{c_{44}} \tag{50}$$

For $|s|>1$ zone parameters and corresponding traction in (44a) for the negative result in (49a) are discarded, and width of the remaining zone given by the positive result. If the half-space surface is the only constraint on the die, then $s=\pm 1$ defines the onset of tipping about, respectively, the leading and trailing die bases. Comparison of (44b) and (45) shows that assumption (38) uncouples the contact zones in so far as relating contact edge location and width. As (47) shows, coupling is implicit *via* the zone widths themselves.

7. Contact zone maximal values

Setting $y=0$ in (A1a,c) and (A3a,c) (see Appendix A) gives in view of (28), (30a) and (40)

$$\partial_x u_x=\mu\frac{B}{A_\varepsilon}\frac{x}{L}\left(1-\frac{x^2}{L^2}\right)+\frac{M_+}{R}\left(1+\mu^2\frac{B}{A_\varepsilon}\right)\frac{\sigma_i}{c_{44}}\quad(x\in Z_i) \tag{51a}$$

$$\theta=-\frac{\varepsilon\mu N_y B}{\alpha a_\varepsilon A_\varepsilon}\frac{x}{L}\left(1-\frac{x^2}{L^2}\right)+\frac{\varepsilon}{\alpha R}\left(T_{3+}-\mu^2\frac{N_y M_+ B}{a_\varepsilon A_\varepsilon}\right)\frac{\sigma_i}{c_{44}}\quad(x\in Z_i) \tag{51b}$$

Study of (51a) in light of (44a) shows that $(\partial_x u_x<0,\ \partial_x^3 u_x>0)$, i.e., constraint (41) is not satisfied for all $x\in Z_i$. Following Brock (2003, 2004), therefore, a global constraint based on the minimum value of $\partial_x u_x$ is imposed

$$\partial_x^2 u_x(x_i^*)=0,\quad 1+\partial_x u_x(x_i^*)\geqslant 0\qquad(x_i^*\in Z_i) \tag{52}$$

Stationary values of θ in the contact zones follow of course from condition

$$\partial_x\theta(x_i^*)=0\quad(x_i^*\in Z_i) \tag{53}$$

Substitution of (51a), (51b) and (44a) and again invoking (38) reduces the equations in (52) and (53), respectively, to the valid approximations

$$(\lambda_u, \lambda_\theta)[\upsilon + \xi(1+\upsilon)] - \xi^{1+\upsilon} \approx 0, \quad \xi = \frac{x_i^* - L_i^-}{L_i^+ - x_i^*} \tag{54a}$$

$$\lambda_u = \frac{M_+}{S}\left(\mu + \frac{A_\varepsilon}{\mu B}\right), \quad \lambda_\theta = \frac{1}{S}\left(\mu M_+ - \frac{a_\varepsilon A_\varepsilon T_{3+}}{\mu B N_y}\right) \tag{54b}$$

The non-integer polynomial in (54a) has a single positive real root which, after Brock and Georgiadis (2000) and Brock (2003), is obtained for (52) and (53), respectively, as

$$\xi = \frac{-\upsilon}{1+\upsilon}(G_u, G_\theta) \tag{55a}$$

$$\ln(G_u, G_\theta) = \frac{1}{\pi}\int_0^\infty \tan^{-1}\frac{2a_\varepsilon A_\varepsilon \Omega t^{1+\upsilon}}{(\lambda_u, \lambda_\theta)[(1+\upsilon)t - \upsilon] - \mu M_+ t^{1+\upsilon}}\frac{\mathrm{d}t}{t} \tag{55b}$$

The global constraints in (52) and the stationary values θ^* follow, respectively, as

$$1 + \frac{2\mu B}{A_\varepsilon}\left(\upsilon + \frac{1}{1-G_u}\right)\frac{L_i}{L} \geqslant 0 \quad (i = 1, 2) \tag{56a}$$

$$\theta^* \approx -\frac{2\varepsilon\mu N_y B}{\alpha a_\varepsilon A_\varepsilon}\left(\upsilon + \frac{1}{1-G_\theta}\right)\frac{L_i}{L} \quad (i = 1, 2) \tag{56b}$$

Expressions (38) and (49) indicate that (56a) is generally satisfied except as $c \to c_R$. Study of (55b) shows that the right-hand side of (56b) is positive, i.e., θ^* is maximal and contact zone temperature increases. Approximate maximum magnitudes $|\sigma_i^*|$ of the compressive contact zone traction σ_i follow in a similar manner:

$$\xi = -1 - 2\upsilon, \quad \left|\frac{\sigma_i^*}{c_{44}}\right| \approx \frac{2R}{S}\frac{(1+\upsilon)^{1+\upsilon}}{(-\upsilon)^\upsilon}\frac{L_i}{L} \quad (i = 1, 2) \tag{57}$$

It is noted that the root ξ in (57) is an *analytic* result and that, as with (41), contact zone coupling in (56) and (57) is implicit in the contact zone widths given by (49a).

8. Some calculations

Insight into effects of sub-critical sliding speed ($c < c_R$), friction (μ) and intersection of the resultant force $\Re$ line of action with the half-space surface (s) on contact zone formation is obtained in view of (49a) from the contact zone width ratio L_2/L_1. Calculations for the hexagonal material zinc (properties are listed in Appendix B) at room temperature ($T_0 = 296$ K) are given in Tables 1 and 2. The entries indicate that the width ratio appropriately vanishes as $s \to -1$ and becomes unbounded as $s \to 1$. Moreover, when the line of action intersection is nearer to the leading die base ($0 < s < 1$), the width ratio decreases both with increasing friction and

Table 1
Contact zone width ratio L_2/L_1 for $\mu = 0.1$ vs dimensionless line of action intersection location s and dimensionless sliding speed c.

s	$c = 0$	$c = 0.1$	$c = 0.2$	$c = 0.3$	$c = 0.4$	$c = 0.5$	$c = 0.6$	$c = 0.7$	$c = 0.8$
−0.9	0.0948	0.0949	0.0949	0.095	0.0951	0.0952	0.0955	0.0959	0.0966
−0.7	0.2652	0.2652	0.2653	0.2655	0.2657	0.2659	0.2665	0.2672	0.2683
−0.5	0.4376	0.4377	0.4378	0.438	0.4382	0.4384	0.4389	0.4397	0.4408
−0.3	0.6305	0.6302	0.6307	0.6304	0.6305	0.6308	0.6312	0.6318	0.6327
−0.2	0.7396	0.7395	0.7396	0.7397	0.7398	0.74	0.7403	0.7408	0.7415
−0.1	0.8614	0.8615	0.8615	0.8615	0.8615	0.8617	0.8618	0.8621	0.8626
0	1.0	1.0	1.0	1.0	1.0	1.0	1.0	1.0	1.0
0.1	1.1609	1.1608	1.1608	1.1607	1.1607	1.1605	1.1603	1.1599	1.1593
0.2	1.3521	1.3522	1.352	1.3519	1.3517	1.3514	1.3508	1.3499	1.3486
0.3	1.5861	1.5867	1.5856	1.5863	1.586	1.5853	1.5843	1.5827	1.5805
0.5	2.2851	2.2845	2.2843	2.2832	2.2823	2.2808	2.2782	2.2744	2.2684
0.7	3.7712	3.7704	3.7687	3.7665	3.7643	3.7605	3.7529	3.743	3.7267
0.9	10.547	10.542	10.536	10.525	10.519	10.502	10.467	10.422	10.349

Table 2
Contact zone width ratio L_2/L_1 for $\mu = (0.1, 0.2, 0.5)$ and $c = (0.2, 0.5)$ vs dimensionless line of intersection location s

s	$c = 0.2$			$c = 0.5$		
	$\mu = 0.1$	$\mu = 0.2$	$\mu = 0.5$	$\mu = 0.1$	$\mu = 0.2$	$\mu = 0.5$
−0.9	0.0949	0.0968	0.1019	0.0952	0.0976	0.104
−0.7	0.2653	0.2686	0.2784	0.2659	0.2699	0.2816
−0.5	0.4378	0.4412	0.4511	0.4384	0.4426	0.4543
−0.3	0.6303	0.633	0.6409	0.6308	0.6341	0.6434
−0.2	0.7396	0.7417	0.7477	0.74	0.7426	0.7496
−0.1	0.8615	0.8626	0.8661	0.8617	0.8631	0.8672
0	1.0	1.0	1.0	1.0	1.0	1.0
0.1	1.1608	1.1593	1.1546	1.1605	1.1586	1.1531
0.2	1.352	1.3483	1.3375	1.3514	1.3467	1.334
0.3	1.5866	1.5798	1.5603	1.5853	1.5771	1.5542
0.5	2.2843	2.2665	2.2169	2.2808	2.2596	2.2042
0.7	3.7687	3.7231	3.5921	3.7605	3.7045	3.5517
0.9	10.536	10.327	9.8162	10.502	10.245	9.5394

increasing sliding speed. If the intersection is nearer to the trailing base ($-1 < s < 0$), there is a decrease both with friction and speed. In both instances, variation with friction is more pronounced.

For insight into solution behavior in the contact zones, locations of the maximum temperature change and maximum compressive stress in the zones are compared. These follow, respectively, from (54a), (55a) and (57) as

$$s_\theta^* = \frac{1}{L_1}(x_1^* + L) = \frac{1}{L_2}(x_2^* - L) \approx -\upsilon - \frac{1+\upsilon}{1+\upsilon(1-G_\theta)} \tag{58a}$$

$$s_\sigma^* = \frac{1}{L_1}(x_1^* + L) = \frac{1}{L_2}(x_2^* - L) \approx -1 - 2\upsilon \tag{58b}$$

Calculations of (58) based on zinc at room temperature are given in Table 3. The negative values show that the maximum compression and temperature increase locations always trail the die base, and that the lag for compression is much larger than that for temperature increase. Both lags increase significantly with increasing friction. For a given friction level, the lag for maximum compression location tends to increase with sliding speed. The lag for location of maximum temperature, however, increases only until speeds near the Rayleigh limit ($c_R = 0.8883$), when it decreases.

For insight into contact zone thermal response, (56b) and (57) are combined to give the maximum temperature increase achieved when the maximum compressive stress in the same zone reaches a given value σ_i^*

Table 3
Dimensionless location (s_θ^*, s_σ^*) with respect to indentor baseline of maximum temperature increase and maximum compression in contact zone vs dimensionless sliding speed c for $\mu = (0.1, 0.2, 0.5)$

c	$\mu = 0.1$		$\mu = 0.2$		$\mu = 0.5$	
	s_θ^*	s_σ^*	s_θ^*	s_σ^*	s_θ^*	s_σ^*
0	−0.0079	−0.0142	−0.0158	−0.0284	−0.0395	−0.071
0.1	−0.0081	−0.0144	−0.0159	−0.0286	−0.0397	−0.0714
0.2	−0.0083	−0.0148	−0.0164	−0.0294	−0.0409	−0.0732
0.3	−0.0087	−0.0154	−0.0172	−0.0306	−0.0428	−0.0762
0.4	−0.0092	−0.0162	−0.0185	−0.0326	−0.0456	−0.0808
0.5	−0.01	−0.0176	−0.0199	−0.0352	−0.0497	−0.0878
0.6	−0.0111	−0.0198	−0.022	−0.0394	−0.0521	−0.0978
0.7	−0.0118	−0.0228	−0.0236	−0.0456	−0.0582	−0.113
0.8	−0.0075	−0.028	−0.0151	−0.056	−0.0372	−0.1382

Table 4
Parameter for maximum contact zone temperature increase θ^* for $\mu = (0.1, 0.2, 0.5)$ vs dimensionless sliding speed c

c	$\frac{c_{44}}{\sigma_i^*}\theta^*$(K), $\mu = 0.1$	$\frac{c_{44}}{\sigma_i^*}\theta^*$(K), $\mu = 0.2$	$\frac{c_{44}}{\sigma_i^*}\theta^*$(K), $\mu = 0.5$
0	279.94	279.9	279.58
0.1	276.81	278.94	279.06
0.2	276.3	278.39	277.63
0.3	274.77	274.72	275.19
0.4	269.51	271.36	271.36
0.5	267.23	265.42	266
0.6	256.68	256.6	256.64
0.7	240.74	240.64	240.83
0.8	196.14	196.49	198.08

$$\frac{c_{44}}{\sigma_i^*}\theta^* \approx \frac{\varepsilon\mu B}{\alpha a_\varepsilon A_\varepsilon}\frac{N_y S}{R}\frac{(-\upsilon)^\upsilon}{(1+\upsilon)^{1+\upsilon}}\left(\upsilon + \frac{1}{1-G_\theta}\right) > 0 \tag{59}$$

The uncoupling effects of (38) are reflected in the presence of σ_i^* as the only zone-specific parameter. Some values for the right-hand side of (59) are given for zinc at room temperature in Table 4 for various friction levels and sliding speeds. Variation with μ is seen to be, in fact, nominal, but an inverse variation with c occurs, and is somewhat more pronounced.

9. Formulation outline for the general case

While illustrative, the two-zone contact case assumed that both die bases exhibit the same friction coefficient, and that a single polynomial function for the die profile can be generated. For the general case $n > 1$ depicted in Fig. 1 it is likely that a polynomial of a very high order would be required. Perhaps a Fourier series could be employed and, indeed, a periodic die profile might require only a single term. Eq. (39), however, suggests an *alternative* approach that (a) does not require periodicity, and (b) allows the use of polynomials that lend themselves to integration processes that can be performed analytically using contour integration and Cauchy's theorem. To complete the present analysis, key steps in formulating this more general case are outlined here.

Returning to Fig. 1, we assume that the normal force system applied to the die can be described as a purely compressive line load over the upper (horizontal) edge of the shaded region. One can therefore locate the origin of the translating coordinates directly under the left-most point, so that the line load function can be written as $f(x) > 0$. The same coordinate system can also be used to locate the lower-most points $x = x_i$ $(i = 1, 2, \ldots, n)$ along the die profile and the upper-most points $x = x_i'$ $(i = 1, 2, \ldots, n-1)$ between two adjacent low points, i.e., $x_i < x_i' < x_{i+1}$. The resultants appearing in (39) can thus be written as

$$F_k = \int_{x_{k-1}'}^{x_k'} f(t)\,\mathrm{d}t \;\; (k = 2, 3 \ldots n-1), \quad F = \int_0^W f(t)\,\mathrm{d}t, \quad M_0 = \int_0^W f(t)t\,\mathrm{d}t \tag{60}$$

Parameter W is the width of the upper edge of the shaded region, and static equivalency allows (39b) and (39c) to be replaced by extending (39d) to include the cases $k = (1, n)$, where

$$F_1 = \int_0^{x_1'} f(t)\,\mathrm{d}t, \quad F_n = \int_{x_{n-1}'}^W f(t)\,\mathrm{d}t \tag{61}$$

We also assume that contact will take place in single zones about each low point $x = x_i$ $(i = 1, 2, \ldots, n)$, i.e., $x_i \in Z_i$, and that it is possible to find polynomials

$$\frac{\mathrm{d}V_i}{\mathrm{d}x} \approx \sum_1^m p_{ik}(x - x_i)^{k-1} \quad (i = 1, 2, \ldots, n) \tag{62}$$

of order $m \geqslant 1$ that accurately represent the die profile in each contact zone.

If $m = 2$, for example, is deemed sufficient for all n zones, then contour integration and Cauchy's theorem can be used with (39a), (39d) and (61) to give

$$L_i = \sqrt{\frac{2S_i \sin \pi\upsilon_i}{\pi\upsilon_i(1+\upsilon_i)R}}\sqrt{\frac{F_i}{p_{i2}c_{44}}}, \quad \widetilde{L}_i = x_i - \frac{p_{i1}}{p_{i2}} - \left(\frac{1}{2}+\upsilon_i\right)L_i \qquad (i = 1,2,\ldots,n). \tag{63}$$

Eqs. (23c) and (32) hold, and it is noted that the die curvatures that arise in the contact zones of Fig. 1 require that $p_{i2} < 0$ $(i = 1,2,\ldots,n)$. Eq. (63) can then be solved for the contact edge location parameters $L_i^{\pm}$. Condition $f(x) > 0$ guarantees that $F_i > 0$. Tipping would occur if $f(x) \leqslant 0$ in continuous regions at the leading or trailing edge of the upper die surface depicted in Fig. 1 and, appropriately, (63) for a zone can be discarded when $F_i \leqslant 0$, i.e., contact does not occur about the corresponding low point of the die profile. In regard to the unilateral constraints (40) and (41) and maximal value results corresponding to (52–57), it is noted that formulas have been worked out for single-zone sliding contact by a parabolic die on transversely isotropic and isotropic half-spaces, respectively, in Brock (2003) and in Brock and Georgiadis (2000). In the interest of brevity, these are not reproduced here.

10. Concluding remarks

1. An exact integral-transform solution for the dynamic steady state response in plane strain of a coupled thermoelastic transversely isotropic half-space to the motion of $n > 1$ zones of surface traction over the surface was given. The thermoelastic model encompassed two special cases of thermal relaxation, and speed was subsonic.
2. Asymptotic forms were extracted and transform inversions given. These were analytic, and depended on a three-category characterization of transverse isotropy similar to a scheme employed for the isothermal case. They were used to obtain a candidate for the exact solution to the mixed boundary value problem of $n > 1$ contact zones formed by a sliding rigid die in the presence of friction.
3. Imposing the auxiliary requirement of non-singular behavior in contact zones led to n equations for the $2n$ contact zone location and width parameters. The other n equations arose by specifying the resultant force and moment exerted on the die, and how that resultant force is actually distributed. Because the die is rigid and does not itself accelerate, this force system is transmitted directly to the half-space surface through the contact zones. Traction distribution was not assumed, but obtained analytically as a quadrature of the die profile function. Thus, the n conditions were linear relations of the force system and such quadratures. Based on a typical assumption (see e.g., Kuznetsov, 1985; Nosnovsky and Adams, 2000) that any contact zone width is much smaller than the separation between any two adjacent zones, robust approximations for these $2n$ quadratures could be written in forms that exhibited the unknown zone width/location parameters only in the profile function itself.
4. As an illustration of their use, a die with two bases was treated. It was assumed that contact occurred around each base, so that the pertinent regularity conditions along with the resultant force conditions were sufficient to derive the four equations necessary to determine contact zone parameters. Use of the tractable approximations of these produced a partly uncoupled set of equations for all the parameters that could be solved algebraically.
5. Results showed that the contact zones indeed form around each base of the die, so long as the line of action of the resultant force exerted by the die passed between the bases. If it passes through one zone, then the other zone vanishes, i.e., if the half-space is the only constraint on the die, this situation represents the onset of tipping.
6. The results also satisfied the unilateral constraint of non-tensile contact and negative frictional work rate for sub-critical (sub-Rayleigh) sliding speeds. Calculations for the hexagonal material zinc at room temperature showed that the nature of the variation of relative contact zone width with friction and sliding speed is especially sensitive to resultant die force line of action. The locations in each contact zone of points of maximum compressive stress and maximum temperature increase varied markedly with sliding speed and friction, but always lay behind the die base.

7. To complete the analysis, a formulation for the general case $n > 1$ was presented, that assumed that the die profile can accurately be represented by polynomial functions in the most likely (lower-most) contact zone sites. For the case of quadratic profile functions, equations for the width and location of the center of each contact zone were presented.
8. The asymptotic analysis valid for $|x/h| \gg 1$, which case for most engineering materials corresponds to the interval $O(10^{-6}\,\mathrm{m}) < |x| < \infty$, showed that there are no thermal relaxation effects in this length scale. Such effects could become appreciable when much smaller length scales are considered.
9. The two-zone case results showed that the additional (often plausible) assumption that contact zone width is much smaller than contact zone separation yields a tractable set of equations that might be solved algebraically for all contact zone width/location parameters. Such an assumption is typical for a rigid die (see e.g., Kuznetsov, 1985) and, in the present analysis, also led to algebraic formulas for locations and values of maximum compressive stress and contact zone temperature increase.
10. Certainly, the approach adopted here is more daunting than such in classical efforts (Kuznetsov, 1985). However, the present approach leads to useful results even when assumptions about thermomechanical behavior and specific zone-size are not warranted.

Acknowledgements

This paper is a partial result of the Project PYTHAGORAS II/EPEAEK II (Operational Programme for Educational and Vocational Training II) [Title of the individual program: 'Micro-mechanics of contacts and diffusion of humidity in granular geomaterials']. This Project is co-funded by the European Social Fund (75%) of the European Union and by National Resources (25%) of the Greek Ministry of Education.

Appendix A

For Category 1 and 2 ($0 < c < 1$) and Category 3 ($c_0 < c < 1$), asymptotic solutions for $y > 0$ are obtained by inversion of transform (22) and counterparts for $(p\hat{u}_y, \hat{\theta})$ as

$$\partial_x u_x = \frac{1}{2\pi\omega R}\sum_i^n \int_{Z_i} \frac{\sigma_{\mathrm{N}}^i}{c_{44}}\left(\frac{N_B B' y}{\tau^2 + B'^2 y^2} - \frac{N_A A' y}{\tau^2 + A'^2 y^2}\right) \mathrm{d}t + \frac{B}{2\pi\omega R}\sum_i^n \int_{Z_i} \frac{\sigma_{\mathrm{S}}^i}{c_{44}}\left(\frac{U_A \tau}{\tau^2 + B'^2 y^2} - \frac{U_B \tau}{\tau^2 + A'^2 y^2}\right) \mathrm{d}t \tag{A.1a}$$

$$\partial_x u_y = \frac{A_\varepsilon}{2\pi\omega R}\sum_i^n \int_{Z_i} \frac{\sigma_{\mathrm{N}}^i}{c_{44}}\left(\frac{U_A \tau}{\tau^2 + A'^2 y^2} - \frac{U_B \tau}{\tau^2 + B'^2 y^2}\right) \mathrm{d}t + \frac{1}{2\pi\omega R}\sum_i^n \int_{Z_i} \frac{\sigma_{\mathrm{S}}^i}{c_{44}}\left(\frac{N_A B' y}{\tau^2 + B'^2 y^2} - \frac{N_B A' y}{\tau^2 + A'^2 y^2}\right) \mathrm{d}t \tag{A.1b}$$

$$\theta = \frac{\varepsilon}{2\alpha\omega}\frac{1}{\pi R}\sum_i^n \int_{Z_i} \frac{\sigma_{\mathrm{N}}^i}{c_{44}}\left(\frac{K_A B' y}{\tau^2 + B'^2 y^2} - \frac{K_B A' y}{\tau^2 + A'^2 y^2}\right) \mathrm{d}t + \frac{\varepsilon}{2\alpha\omega}\frac{B}{\pi R}\sum_i^n \int_{Z_i} \frac{\sigma_{\mathrm{S}}^i}{c_{44}}\left(\frac{T_A \tau}{\tau^2 + A'^2 y^2} - \frac{T_B \tau}{\tau^2 + B'^2 y^2}\right) \mathrm{d}t. \tag{A.1c}$$

In addition to those defined in (23a), (23b) and (A1) exhibits the terms

$$\tau = t - x \tag{A.2a}$$

$$(K_A, K_B) = N_x B(A', B') - M_y A_\varepsilon(B', A') \tag{A.2b}$$

$$(T_A, T_B) = M_x B^2 - N_y(A'^2, B'^2) \tag{A.2c}$$

For Category 3 ($0 < c < c_0$) results for $y > 0$ are

$$\begin{aligned}\partial_x u_x = {} & \frac{M_+}{2\pi R}\sum_i^n \int_{Z_i} \frac{\sigma_{\mathrm{N}}^i}{c_{44}}\left(\frac{\Omega y}{\tau_+^2+\Omega^2 y^2}+\frac{\Omega y}{\tau_-^2+\Omega^2 y^2}\right)\mathrm{d}t \\ & + \frac{M_-}{2\pi R}\frac{\Omega}{\bar\omega}\sum_i^n \int_{Z_i} \frac{\sigma_{\mathrm{N}}^i}{c_{44}}\left(\frac{\tau_-}{\tau_-^2+\Omega^2 y^2}-\frac{\tau_+}{\tau_+^2+\Omega^2 y^2}\right)\mathrm{d}t \\ & + \frac{BK}{4\pi\bar\omega R}\sum_i^n \int_{Z_i} \frac{\sigma_{\mathrm{S}}^i}{c_{44}}\left(\frac{\Omega y}{\tau_-^2+\Omega^2 y^2}-\frac{\Omega y}{\tau_+^2+\Omega^2 y^2}\right)\mathrm{d}t \\ & - \frac{a_\varepsilon B\Omega}{\pi R}\sum_i^n \int_{Z_i} \frac{\sigma_{\mathrm{S}}^i}{c_{44}}\left(\frac{\tau_+}{\tau_+^2+\Omega^2 y^2}+\frac{\tau_-}{\tau_-^2+\Omega^2 y^2}\right)\mathrm{d}t \end{aligned} \tag{A.3a}$$

$$\begin{aligned}\partial_x u_y = {} & \frac{M_+}{2\pi R}\sum_i^n \int_{Z_i} \frac{\sigma_{\mathrm{N}}^i}{c_{44}}\left(\frac{\Omega y}{\tau_+^2+\Omega^2 y^2}+\frac{\Omega y}{\tau_-^2+\Omega^2 y^2}\right)\mathrm{d}t \\ & + \frac{M_-}{2\pi R}\frac{\Omega}{\bar\omega}\sum_i^n \int_{Z_i} \frac{\sigma_{\mathrm{N}}^i}{c_{44}}\left(\frac{\tau_-}{\tau_-^2+\Omega^2 y^2}-\frac{\tau_+}{\tau_+^2+\Omega^2 y^2}\right)\mathrm{d}t \\ & + \frac{A_\varepsilon K}{4\pi\bar\omega R}\sum_i^n \int_{Z_i} \frac{\sigma_{\mathrm{S}}^i}{c_{44}}\left(\frac{\Omega y}{\tau_-^2+\Omega^2 y^2}-\frac{\Omega y}{\tau_+^2+\Omega^2 y^2}\right)\mathrm{d}t \\ & + \frac{a_\varepsilon A_\varepsilon \Omega}{\pi R}\sum_i^n \int_{Z_i} \frac{\sigma_{\mathrm{S}}^i}{c_{44}}\left(\frac{\tau_-}{\tau_-^2+\Omega^2 y^2}+\frac{\tau_+}{\tau_+^2+\Omega^2 y^2}\right)\mathrm{d}t \end{aligned} \tag{A.3b}$$

$$\begin{aligned}\theta = {} & -\frac{\varepsilon}{\alpha}\frac{T_{3+}}{2\pi R}\sum_i^n \int_{Z_i} \frac{\sigma_{\mathrm{N}}^i}{c_{44}}\left(\frac{\Omega y}{\tau_+^2+\Omega^2 y^2}+\frac{\Omega y}{\tau_-^2+\Omega^2 y^2}\right)\mathrm{d}t \\ & + \frac{\varepsilon\Omega}{\alpha\bar\omega}\frac{T_{3-}}{2\pi R}\sum_i^n \int_{Z_i} \frac{\sigma_{\mathrm{S}}^i}{c_{44}}\left(\frac{\tau_-}{\tau_-^2+\Omega^2 y^2}-\frac{\tau_+}{\tau_+^2+\Omega^2 y^2}\right)\mathrm{d}t \end{aligned} \tag{A.3c}$$

In addition to those defined in (23a), (23b) and (A3) exhibits the terms

$$\tau_\pm = t - x \pm \bar\omega y \tag{A.4a}$$

$$K = (m_\varepsilon - 1)^2 - a_\varepsilon^2 A_\varepsilon^2 - c^2 \tag{A.4b}$$

$$T_{3\pm} = N_x B \pm M_y A_\varepsilon, \quad M_\pm = a_\varepsilon A_\varepsilon \pm (1 - m_\varepsilon)B \tag{A.4c}$$

It is noted that (A1) and (A3) coincide when either $c \to c_0$ or $y = 0$.

Appendix B

Properties of the hexagonal material zinc at room temperature are given by Sharma and Sharma (2002)

$c_{11} = 162.8$ GPa, $c_{22} = 62.7$ GPa, $c_{44} = 38.5$ GPa, $c_{12} = 50.8$ GPa, $c_{13} = 36.2$ GPa

$\rho = 7140\ \mathrm{kg/m^3}$

$T_0 = 296$ K, $c_v = 390\ \mathrm{J/kg\,m}$, $K_x = K_y = 124\ \mathrm{W/m\,K}$

$\alpha_x = 5.818(10^{-6})\ 1/\mathrm{K}$, $\alpha_y = 15.35(10^{-6})\ 1/\mathrm{K}$

In view of (26) and (27), these values give the dimensionless Category 3 speed and dimensionless Rayleigh-wave speed in the plane of material symmetry as, respectively, $c_0 = 0.999$ and $c_{\mathrm{R}} = 0.8883$.

References

Abramowitz, M., Stegun, I.A., 1972. Handbook of Mathematical Functions. Dover, New York.
Achenbach, J.D., 1973. Wave Propagation in Elastic Solids. North-Holland, Amsterdam.

Berg, L., 1967. Introduction to the Operational Calculus. North-Holland, Amsterdam.
Boley, B.A., Weiner, J.H., 1985. Theory of Thermal Stresses. Krieger, Malabar, FL.
Bracewell, R., 1965. The Fourier Transform and Its Applications. McGraw-Hill, New York.
Brock, L.M., 2003. Rapid sliding indentation with friction on a transversely isotropic thermoelastic half-space. Int. J. Solids Structures 40, 3195–3219.
Brock, L.M., 2004. Rolling without slip on a transversely isotropic thermoelastic half-space. J. Elasticity 77, 139–162.
Brock, L.M., Georgiadis, H.G., 1997. Steady-State motion of a line mechanical/heat source over a half-space: a thermoelastodynamic solution. ASME J. Appl. Mech. 64, 562–567.
Brock, L.M., Georgiadis, H.G., 1999. Convection effects for rapidly moving mechanical sources on a half-space governed by fully coupled thermoelasticity. ASME J. Appl. Mech. 66, 347–351.
Brock, L.M., Georgiadis, H.G., 2000. Sliding contact with friction on a thermoelastic solid at subsonic, transonic and supersonic speeds. J. Therm. Stresses 23, 629–656.
Brock, L.M., Georgiadis, H.G., 2001. An illustration of sliding contact at any constant speed on highly elastic half-spaces. IMA J. Appl. Math. 66, 551–566.
Carrier, G.F., Krook, M., Pearson, C.E., 1966. Functions of a Complex Variable. McGraw-Hill, New York.
Chadwick, P.C., 1960. Thermoelasticity – the dynamical theory. In: Sneddon, I.N., Hill, R. (Eds.), Progress in Solid Mechanics, vol. 1. North-Holland, Amsterdam, pp. 265–328.
Chekina, O.G., Keer, L.M., 1999. A new approach to calculation of contact characteristics. ASME J. Tribol. 121, 20–27.
Dhaliwal, R.S., Sherief, H.H., 1980. Generalized thermoelasticity for anisotropic media. Quart. Appl. Math. 38, 1–8.
Erdogan, F., 1976. Mixed boundary value problems in mechanics. In: Nemat-Nasser, S. (Ed.), Mechanics Today, vol. 4. Pergamon Press, New York, pp. 1–86.
Galin, L.A., 1961. Contact problems in the theory of elasticity. North Carolina State College, Department of Mathematics.
Georgiadis, H.G., Barber, J.R., 1993. On the super-Rayleigh/subseismic elastodynamic indentation problem. J. Elasticity 31, 141–161.
Gladwell, G.M.L., 1980. Contact Problems in the Classical Theory of Elasticity. Sijthoff and Noordhoff, Alphen aan Rijn.
Green, A.E., Lindsay, K.A., 1972. Thermoelasticity. J. Elasticity 2, 1–7.
Hills, D.A., Nowell, D., 1994. Mechanics of Fretting Fatigue. Kluwer Academic Publishers., Dordrecht.
Kim, J.S., Kim, K.W., 2002. Effects of distance between pads on the inlet pressure buildup on pad bearings. ASME J. Tribol. 124, 506–514.
Kuznetsov, E.A., 1985. Periodic contact problems for half-plane allowing for forces of friction. Sov. Appl. Mech. 12, 37–44.
Ling, F.F., 1973. Surface Mechanics. Wiley, New York.
Lord, H.W., Shulman, Y., 1967. Generalized dynamical theory of thermoelasticity. J. Mech. Phys. Solids 15, 299–309.
Nosnovsky, M., Adams, G.G., 2000. Steady state frictional sliding of two elastic bodies with a wavy contact surface. ASME J. Tribol. 122, 490–502.
Payton, R.G., 1983. Elastic Wave Propagation in Transversely Isotropic Media. Martinus Nijhoff, The Hague.
Sharma, J.N., Sharma, P.K., 2002. Free vibration analysis of homogeneous transversely isotropic thermoelastic cylindrical panel. J. Therm. Stresses 25, 169–182.
Tabor, D., 1981. Friction – the present state of our understanding. ASME J. Lubr. Tech. 103, 169–179.
Tichy, J.A., Meyer, D.M., 2000. Review of solid mechanics in tribology. Int. J. Solids Structures 37, 391–400.
van der Pol, B., Bremmer, H., 1950. Operational Calculus Based on the Two-sided Laplace Integral. Cambridge University Press, Cambridge.